AIP | Applied Physics Letters

Simulated pressure-induced blue-shift of phase-matching region and nonlinear optical mechanism for K3B6O10X (X=Cl, Br)

Bingbing Zhang, Ming-Hsien Lee, Zhihua Yang, Qun Jing, Shilie Pan, Min Zhang, Hongping Wu, Xin Su, and Cheng-Shun Li

Citation: Applied Physics Letters **106**, 031906 (2015); doi: 10.1063/1.4906427
View online: http://dx.doi.org/10.1063/1.4906427
View Table of Contents: http://scitation.aip.org/content/aip/journal/apl/106/3?ver=pdfcov
Published by the AIP Publishing

Simulated pressure-induced blue-shift of phase-matching region and nonlinear optical mechanism for $K_3B_6O_{10}X$ (X = Cl, Br)

Bingbing Zhang (张兵兵),[1,2] Ming-Hsien Lee (李明憲),[1,3] Zhihua Yang (杨志华),[1,a)] Qun Jing (井群),[1] Shilie Pan (潘世烈),[1,a)] Min Zhang (张敏),[1] Hongping Wu (吴红萍),[1] Xin Su (苏欣),[1,2] and Cheng-Shun Li (李政勛)[3]

[1]*Key Laboratory of Functional Materials and Devices for Special Environments of CAS, Xinjiang Key Laboratory of Electronic Information Materials and Devices, Xinjiang Technical Institute of Physics and Chemistry of CAS, 40-1 South Beijing Road, Urumqi 830011, China*

[2]*University of Chinese Academy of Sciences, Beijing 100049, China*

[3]*Department of Physics, Tamkang University, New Taipei City 25137, Taiwan*

(Received 17 December 2014; accepted 10 January 2015; published online 22 January 2015)

Birefringence plays a great role in phase matching of the nonlinear optical (NLO) crystals. Small birefringence restricts various crystals from achieving deep-ultraviolet laser output although they exhibit short UV cutoff edges and high second-harmonic generation (SHG) intensities. An access to achieve deeper coherent light output through external pressure on NLO crystal, $K_3B_6O_{10}Cl$ is proposed and demonstrated through computer experiment based on the first principles theory. The "hot spot" in structure that determine the SHG effects and birefringence were highlighted. The shortest achievable phase-matching wavelengths are predicted based on calculated refractive indices. It is found that the quasi-planar $(B_6O_{10})^{2-}$ group is the dominant contributing unit to optical anisotropy. The pressure-induced increase of polarizability anisotropy of $(B_6O_{10})^{2-}$ group can notably enlarge birefringence which extends the shortest achievable wavelength of $K_3B_6O_{10}Cl$ frequency conversion. The results show that pressure engineering may be a promising scheme to overcome the drawback of small birefringence of some NLO crystals. © *2015 AIP Publishing LLC*. [http://dx.doi.org/10.1063/1.4906427]

Nonlinear optical (NLO) crystals are the key materials to extend the working wavelength range of solid state laser through frequency conversion and drive wide applications in many fields.[1,2] As the continuous development of laser micromaching, laser communication, and modern scientific instrument (e.g., laser-based photoemission spectroscopy), the ultraviolet/deep-ultraviolet (UV/DUV) NLO crystals are increasingly required.[3–6] However, the exploration of DUV NLO crystals is a great challenge because of rigorous prerequisites that include a wide transparency window down to the DUV spectral region, a large second-harmonic generation (SHG) effects and a sufficient birefringence to achieve phase matchability. Consequently, the exploration of DUV NLO materials exclusively limited within borates system which possess both wide transparency and large SHG effects. Over the past decades, continuous intensive studies have resulted in the discovery of various NLO materials, such as β-BaB_2O_4 (BBO),[7] LiB_3O_5 (LBO),[8] CsB_3O_5 (CBO),[5] $CsLiB_6O_{10}$ (CLBO),[9] $KBe_2BO_3F_2$ (KBBF) families,[10] $MM'Be_2B_2O_6F$ (M = Na, M′ = Ca; M = K, M′ = Ca, Sr),[11] $NaBeB_3O_6$ (NBBO) families,[12] $NaSr_3Be_3B_3O_9F_4$,[13] $Sr_2Be_2B_2O_7$ (SBBO),[14] $Ba_4B_{11}O_{20}F$,[4] and $Li_4Sr(BO_3)_2$.[15] Among them, KBBF is the only practically usable DUV material to date that satisfy the criteria mentioned above and can generates coherent light of wavelength below 200 nm by the direct SHG. Unfortunately, KBBF is very poisonous and features a strong layer growth habit.[6] Besides KBBF, various materials exhibit short UV cutoff edges and high SHG intensities. Typical examples include SrB_4O_7,[16] BPO_4, LBO, CBO, and CLBO with UV cutoff edges of 120, 134, 160, 167, and 175 nm and SHG intensities of 8×, 2×, 3×, 2.5× and 2.7× KH_2PO_4 (KDP), respectively. However, their relative smaller birefringence's compared to that of KBBF cause them impossible to satisfy the phase-matching condition in the DUV region. This shows birefringence plays a great role in phase matching of the NLO crystals. Therefore, it is meaningful to study optical anisotropy properties of NLO materials and accordingly propose the method that can help us to enlarge the birefringence and further achieve DUV output.

Recently, our group found a borate halide NLO material series $K_3B_6O_{10}X$ (X = Cl, Br)[17–19] that exhibits a large SHG response and short wavelength UV cutoff edges (180 nm). These results highlight $K_3B_6O_{10}X$ (X = Cl, Br) as a promising material series for NLO materials. However, until now, there is no deep insight into the mechanism of NLO properties that is crucial to help us to improve the NLO properties of the corresponding crystals. In this work, we systematically analysis the NLO properties of $K_3B_6O_{10}Cl$ (KBOC) and its isostructure $K_3B_6O_{10}Br$ (KBOB) based on the first-principles theory. The "hot spot" that cause optical anisotropy and further determine the shortest achievable phase-matching wavelength were highlighted. Accordingly, an access to achieve DUV coherent light output through external pressure is proposed based on simulated experiment.

SHG tensor is a very important parameter to characterize NLO property. Started in the 1960s, some groups greatly improved the evaluation methods to calculate SHG tensor from the band structure.[20–22] Aversa and Sipe[21] used the length-gauge in their derivation to give expressions free from the unphysical divergence in the static limit.

a)Electronic addresses: zhyang@ms.xjb.ac.cn and slpan@ms.xjb.ac.cn

Afterward, Rashkeev *et al.*[22] rearranged the equations to make Kleinman symmetry of SHG tensor more apparent. Lin *et al.*[23] further rearranged Rashkeev's zero-frequency formula into Virtual-Hole (VH), Virtual-Electron (VE), and Two-Bands (TB) contributions. It became more compact and shows Kleinman symmetry more explicitly with its full permutation indexes. The energy eigenvalues that appear as differences in denominators are now separated by band gap, the fact that no divergence could occur for insulator is therefore transparent. The formula has been used to predict the SHG coefficients of a large number of crystals.[2] It has been noticed that in these early works the contribution from the Two-Bands process is so small that can be neglected. Incidentally, we were able to prove that Two-Bands term cancel exactly[24] (the detail is given in the supplementary material[25]). The long-term suspicions of why Two-Bands contribution in SHG is so small compared with the other two (VE and VH) is finally settle down. In the present work, we use the following formula for calculating the SHG coefficients:

$$\chi^{(2)}_{\alpha\beta\gamma} = \chi^{(2)}_{\alpha\beta\gamma}(\mathrm{VE}) + \chi^{(2)}_{\alpha\beta\gamma}(\mathrm{VH}), \tag{1}$$

$$\chi^{(2)}_{\alpha\beta\gamma}(\mathrm{VE}) = \frac{e^3}{2\hbar m^3}\sum_{vcc'}\int\frac{d^3k}{4\pi^3}P(\alpha\beta\gamma)\mathrm{Im}\left[P^{\alpha}_{cv}P^{\beta}_{cc'}P^{\gamma}_{c'v}\right] \times\left(\frac{1}{\omega^3_{cv}\omega^2_{vc'}}+\frac{2}{\omega^4_{vc}\omega_{c'v}}\right), \tag{2}$$

$$\chi^{(2)}_{\alpha\beta\gamma}(\mathrm{VH}) = \frac{e^3}{2\hbar m^3}\sum_{vv'c}\int\frac{d^3k}{4\pi^3}P(\alpha\beta\gamma)\mathrm{Im}\left[P^{\alpha}_{vv'}P^{\beta}_{cv'}P^{\gamma}_{cv}\right] \times\left(\frac{1}{\omega^3_{cv}\omega^2_{v'c}}+\frac{2}{\omega^4_{vc}\omega_{cv'}}\right). \tag{3}$$

Here, α, β, and γ are Cartesian components, v and v' denote valence bands, c and c' denote conduction bands, and $P(\alpha\beta\gamma)$ denotes full permutation. The band energy difference and momentum matrix elements are denoted as $\hbar\omega_{ij}$ and $P_{ij}{}^{\alpha}$, respectively.

The electronic and band structures as well as linear optical property calculations were performed by employing CASTEP,[26] a plane-wave pseudopotential density functional theory (DFT) package, with the norm-conserving pseudopotentials (NCP).[27] The exchange-correlation functional was Perdew-Burke-Emzerhoff (PBE) functional within the generalized gradient approximation (GGA).[28] The plane-wave energy cutoff was set at 900.0 eV. Self-consistent field (SCF) calculations were performed with a convergence criterion of 0.5×10^{-6} eV/atom on the total energy. The k-point separation for each material was set as 0.025 Å^{-1} in the Brillouin zone, resulting in corresponding Monkhorst-Pack k-point meshes $6\times6\times6$. There are 168 empty bands (3 times of valence bands) involved in the calculation to ensure the convergence of SHG coefficients.

KBOC and KBOB crystallize in the rhombohedral space group R3m. As shown in Figure 1, the structure of the KBOC crystal is composed of two networks. The first one is the $[B_6O_{10}]_\infty$ network connected by hexaborate B_6O_{13} units through their vertices. The second one is the ClK_6 network, in which the ClK_6 units are linked together through sharing potassium atoms to create a perovskite framework. The whole structure is analogous to the mineral perovskite $CaTiO_3$, the B_6O_{13} units occupy the positions of the calcium cations, and the ClK_6 octahedra are similar to the TiO_6 octahedra.

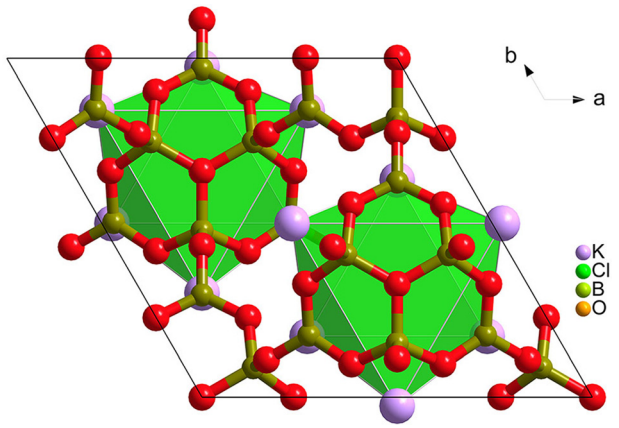

FIG. 1. The 3D framework of KBOC along c direction with B_6O_{13} unit and ClK_6 units.

The band structures of KBOC and KBOB calculated along selected high symmetry k-points within GGA using the first-principles method are similar to each other due to their isomorphic structures. They are both direct gap materials with calculated band gaps of 5.31 and 5.26 eV, which are relatively smaller than experimental band gaps (6.8 and 6.4 eV) resulting from discontinuity of exchange-correlation energy functional. These differences will be corrected using a so-called scissors energy shift when evaluating optical properties based on DFT band structure calculation results.

Using Eq. (1), the SHG coefficients of KBOC and KBOB are calculated from band wave functions. The KBOC and KBOB belong to C_{3v} point group and, owning to symmetry restriction, there are three independent elements: d_{22}, d_{31}, and d_{33}. The calculated results are listed in Table I. The largest tensor component is d_{22}, which is about 2.6 and 3 times that of KDP ($(|d_{36}(1064\,\text{nm})| = 0.39\,\text{pm/V})$ for KBOC and KBOB, respectively. d_{31} is very small for both KBOC and KBOB. Zhang *et al.*[19] and Xia *et al.*[29] measured the SHG coefficients of KBOB using Maker fringe method, as listed in Table I. One can find that the calculated results are in well agreement with the experimental ones in both absolute value and relative order.

To investigate the respective contribution of each electron state at spectral representation and identify the NLO-active units at spatial distribution, the band-resolved[30] and SHG-density[31] methods are adopted here. The biggest tensor d_{22} is analyzed and the results are drawn in Figure 2. In valence bands, the non-bonding $2p$ orbitals of oxygen

TABLE I. Calculated SHG coefficients with a correction of the band gap by using a scissor operator of KBOC and KBOB, and the experimental SHG coefficients measured by Maker fringe method of KBOB (unit: pm/V).

Crystal		d_{22}	d_{33}	d_{31}
KBOC	Present calculation	−1.033	0.488	−0.033
KBOB	Present calculation	−1.169	0.627	0.003
	Expt.[19]	0.83	0.51	Too small
	Expt.[29]	1.23	0.43	Too small

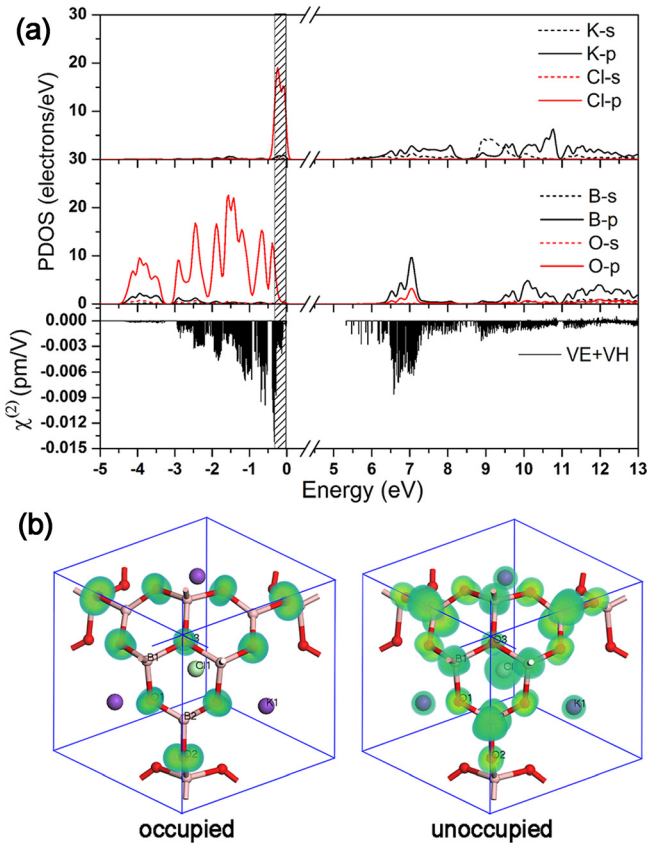

FIG. 2. (a) The partial density of states (PDOS) of KBOC and the band-resolved results of χ_{22}. The diagonal area marks the 3*p* orbitals of chlorine. (b) The non-bonding 2*p* orbitals of oxygen and π anti-bonding orbitals of BO_3 substructure make major contribution to χ_{22} in valence and conduction bands, respectively. The VE process is analyzed using SHG density method because it dominates the SHG in the crystals studied (larger than 94% to both KBOC and KBOB).

make major contribution. In addition, the 3*p* orbitals of chlorine near Fermi level also make an apparent contribution (shown as marked region in Figure 2(a)). As to conduction bands, the NLO-active states disperse in a wide range and the remarkable states located around 7 eV which is characterized by π anti-bonding orbitals composed of 2*p* states of three-fold coordination boron and oxygen.[32] In both occupied and unoccupied states, halogen atoms make significant per-atom contribution. The NLO mechanism of KBOB is similar to that of KBOC. For both KBOC and KBOB, the non-bonding 2*p* orbitals of O atoms in occupied states and the π anti-bonding orbital of BO_3 substructure is the major source. Besides, the per-atom contribution of halogen is significant.

TABLE II. Analysis of the SHG coefficients and birefringence using real-space atom-cutting method (unit in pm/V).

Crystal	Contributions	d_{22}	d_{33}	d_{31}	Δn
KBOC	K^+	−0.023	0.201	−0.060	0.009(ClK_6)
	Cl^-	−0.075	−0.033	0.040	
	$(B_6O_{10})^{2-}$	−0.947	0.438	−0.081	0.047
	Sum	−1.045	0.606	−0.101	…
	Origin	−1.033	0.488	−0.033	0.047
KBOB	K^+	−0.048	0.136	−0.062	0.011(BrK_6)
	Br^-	−0.123	0.098	0.104	
	$(B_6O_{10})^{2-}$	−1.026	0.417	−0.119	0.047
	Sum	−1.197	0.651	−0.077	…
	Origin	−1.169	0.627	0.003	0.049

Table II shows the respective contributions of $(B_6O_{10})^{2-}$ group, K^+ and halogen of KBOC and KBOB using the real-space atom-cutting method. In all SHG contributions to d_{22}, $(B_6O_{10})^{2-}$ is found to be the major origin (90.6% and 85.7% for KBOC and KBOB, respectively). Cl^- and Br^- are the second large source that is about 7.2% and 10.3%, respectively. The contribution of K is very small. As to d_{33} and d_{22}, the contribution of $(B_6O_{10})^{2-}$ becomes small comparing to that in d_{22} due to the restriction of the symmetry[33] of quasi-planar $(B_6O_{10})^{2-}$ and result in the decrease of total value. The changes of the contribution of K^+ and Cl^-/Br^- are small comparing to that in d_{22}. On the whole, $(B_6O_{10})^{2-}$ dominate the large tensors, such as d_{22} and d_{33}, but it does not in small tensor d_{31} due to the restriction of symmetry both in KBOC and KBOB. Br^- exhibit a slightly larger SHG contribution than Cl^- in all the tensors.

Besides NLO effects, a sufficiently large birefringence for phase-matching is another important prerequisity. The calculated dispersion curves of the refractive indices n_e and n_o using DFT method are plotted together with the experimental data[18,19] in Figure 3(a). The calculated results are slightly larger than experimental one. Nevertheless, it shows an excellent agreement between calculation and experiment after slightly shifting the calculated curve down. The results illustrate that DFT method excel at predict birefringence and chromatic dispersion of refractive indices to the title materials and hence the shortest achievable phase-matching wavelength (λ_s), which satisfy $n_o(\lambda) - n_e(\lambda/2) = 0$, simply because λ_s only depends on the birefringence and chromatic dispersion.

KBOC and KBOB exhibit similar birefringence but the former can achieve a shorter phase-matching region. As we know, beside large birefringence, small chromatic dispersion is beneficial to phase-matching. Therefore, the dispersion powers ($dn/d\lambda$) of experimental and predicted refractive indices are calculated. As shown in Figure 3(b), KBOC shows a smaller dispersion power, which causes KBOC reaching a shorter achievable phase-matching wavelength comparing to KBOB. When the band gap of KBOB is shifted up to be equal to KBOC using a scissors operator, the dispersion power decrease and be comparable to that of KBOC. It reveals that the larger band gap of KBOC results in a smaller chromatic dispersion, which further leads to a shorter achievable phase-matching wavelength comparing to KBOB. This identifies KBOC as a better NLO material to achieve a shorter wavelength output comparing to KBOB.

As shown in Table II, $(B_6O_{10})^{2-}$ dominate the contribution to anisotropy, while XK_6 (X = Cl, Br) is small. Therefore, an access to increase the optical anisotropy by changing the structure anisotropy of $(B_6O_{10})^{2-}$ group is proposed. We apply stress along z-direction to KBOC and investigate the variation of its birefringence. The calculated birefringence under various z-direction pressures are given in Figure 3(c). It increases linearly from 0.049 to 0.086 at 700 nm when the z-pressure increases from 0 to 10 GPa. The hydrostatic pressure is also applied. As shown in Figure 3(d),

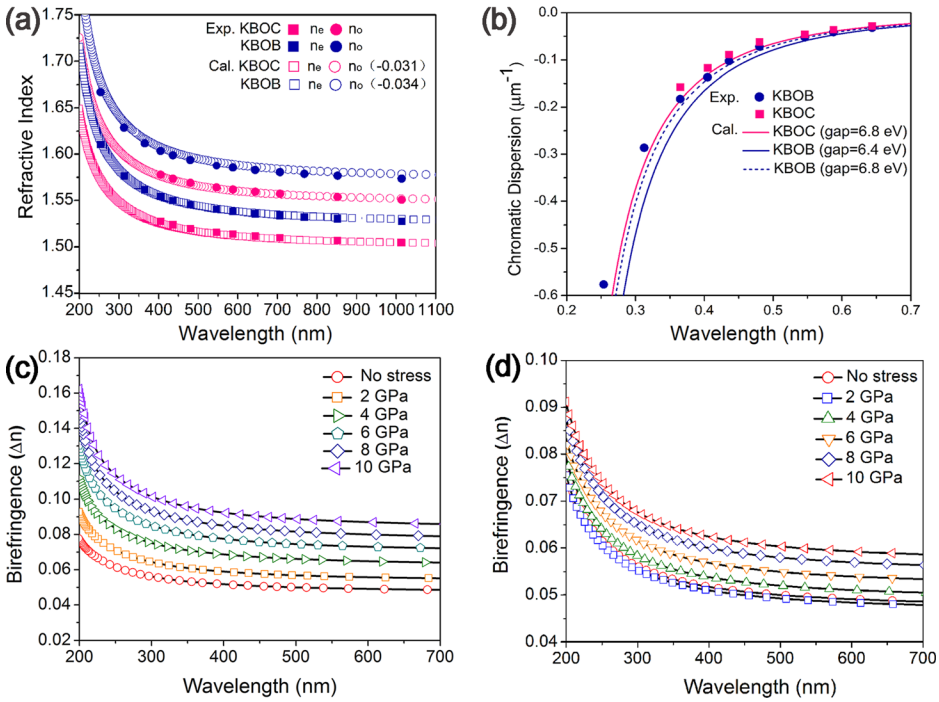

FIG. 3. (a) The experimental and calculated refractive indices of KBOC and KBOB (calculated refractive indices are shifted down by value in bracket). (b) The dispersion powers ($dn/d\lambda$) of experimental and predicted refractive indices of KBOC and KBOB. (c) The calculated birefringence under various pressure along z-direction and (d) hydrostatic pressure.

the birefringence increase, like z-direction pressure mode, with the enhancement of pressure. The calculated birefringence increase from 0.049 to 0.059 at 700 nm when the hydrostatic pressure increase from 0 to 10 GPa. Based on the calculated refractive indices under 10 GPa pressure, the coefficients in Sellmeier equations were fitted (the Sellmeier coefficients are listed in Table SI in the supplemental material[25]) and the phase-matching angles for type I as a function of fundamental wavelength are predicted. As shown in Figure 4, the shortest achievable wavelengths by type I SHG are 216 and 239 nm, which are less than the result predicted without pressure. The pressure strategy can effectively increase the birefringence and accordingly extend the shortest achievable wavelength of KBOC.

According to the well-known Lorentz-Lorenz relationship,[3] the refractive indices are related to the polarizability of materials. To further explore the reason of pressure-induced change of birefringence, we calculated the polarizabilities $\alpha_{//}$ and $\alpha_{\perp}$ of $(B_6O_{13})^{-2}$ group using the DFT method implemented by the Gaussian09 package[34] at 6–31 G level. The calculated results of fragments from zero-pressure and 10 GPa are listed in Figure S1 in the supplementary material.[25] One can define the optical anisotropy as $\delta = \alpha_{\perp} - \alpha_{//}$.[35] The calculated optical anisotropy are $\delta_0 = 11.7$ (no stress), $\delta_h = 14.0$ (10 GPa hydrostatic pressure), and $\delta_z = 23.9$ (10 GPa z-direction pressure), which are proportional to corresponding birefringence of 0.049, 0.059, and 0.086. One can see that the construction of $(B_6O_{13})^{-2}$ group are squashed to become more planar with the increase of pressure. Therefore, the optical anisotropy of the $(B_6O_{13})^{-2}$ increase with structural change under pressure that further results in the increase of birefringence of the crystal.

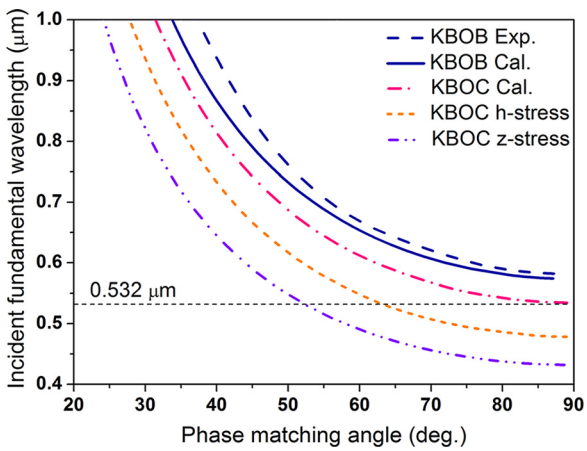

FIG. 4. The phase-matching angles for type I as a function of fundamental wavelength. The predicted shortest achievable phase-matching wavelength of KBOB based on calculated refractive index is in excellent agreement with that of experimental refractive index. The shortest achievable wavelengths of KBOC are obviously blue-shifted (10 GPa hydrostatic pressure, orange; 10 GPa z-direction pressure) compared with non-pressure one.

In summary, the systematically analysis to KBOC and KBOB give a deeper insight into the mechanism of NLO effects based on the first principles theory. The SHG coefficients are calculated by static limit formula. The calculated results are in well agreement with the experimental ones in both absolute value and relative order. The "hot spot" that determine the SHG effects of KBOC and KBOB were highlighted using our band-resolved weighted density method. For both the KBOC and KBOB, the transition between nonbonding 2p orbitals of O atoms in occupied states and the π anti-bonding orbital of BO_3 substructure is the major source. In addition, halogen atoms make significant per-atom contribution. Furthermore, dispersion curves for refractive indices were calculated and then fitted using the Sellmeier equations. Based on this, we predict the shortest achievable phase-matching wavelength of KBOC and further identify KBOC as a better NLO material to achieve a shorter wavelength output comparing to KBOB due to larger band gap of KBOC. The quasi-planar $(B_6O_{10})^{2-}$ group is found to be the dominant contributor to optical anisotropy using atom-cutting analysis method. Based on computer experiment, application of external pressure is proposed to achieve

deeper coherent light output. We also predicted that pressure-induced increase of polarizability anisotropy of $(B_6O_{10})^{2-}$ group can notably enlarge birefringence which extends the shortest achievable wavelength of KBOC. The results show that pressure engineering may be a promising scheme to enlarge birefringence and further achieve deeper coherent light output of some NLO crystals.

This work was supported by National Basic Research Program of China (Grant No. 2014CB648400), the "National Natural Science Foundation of China" (Grant Nos. 11474353, U1129301, and U1303193). Ming-Hsien Lee thanks NCHC for database responses support and Key Win Electronics Co. for equipment donation.

[1]P. Becker, Adv. Mater. **10**(13), 992 (1998).
[2]C. Chen, T. Sasaki, R. Li, Y. Wu, Z. Lin, Y. Mori, Z. G. Hu, J. Wang, S. Uda, M. Yoshimura, and Y. Kaneda, in *Nonlinear Optical Borate Crystals* (Wiley-VCH Verlag & Co. KGaA, 2012).
[3]C. J. F. Boettcher, *Theory of Electric Polarization* (Elsevier, Amsterdam, 1973); Z. Levine, Phys. Rev. B **42**(6), 3567 (1990).
[4]H. Wu, H. Yu, Z. Yang, X. Hou, X. Su, S. Pan, K. R. Poeppelmeier, and J. M. Rondinelli, J. Am. Chem. Soc. **135**(11), 4215 (2013).
[5]Y. Wu, T. Sasaki, S. Nakai, A. Yokotani, H. Tang, and C. Chen, Appl. Phys. Lett. **62**(21), 2614 (1993).
[6]P. Yu, L. M. Wu, L. J. Zhou, and L. Chen, J. Am. Chem. Soc. **136**(1), 480 (2014).
[7]C. Chen, B. Wu, A. Jiang, and G. You, Sci. Sin., Ser. B **28**, 235 (1985), available online at http://chem.scichina.com:8081/sciBe/EN/abstract/abstract396911.shtml.
[8]C. Chen, Y. Wu, A. D. Jiang, B. Wu, G. You, R. Li, and S. Lin, J. Opt. Soc. Am. B **6**(4), 616 (1989).
[9]J.-M. Tu and D. A. Keszler, Mater. Res. Bull. **30**(2), 209 (1995).
[10]C. Chen, Y. Wang, Y. Xia, B. Wu, D. Y. Tang, K. C. Wu, Z. Wenrong, L. Yu, and L. Mei, J. Appl. Phys. **77**(6), 2268 (1995); H. Huang, C. Chen, X. Wang, Y. Zhu, G. Wang, X. Zhang, L. Wang, and J. Yao, J. Opt. Soc. Am. B **28**(9), 2186 (2011).
[11]H. Huang, J. Yao, Z. Lin, X. Wang, R. He, W. Yao, N. Zhai, and C. Chen, Chem. Mater. **23**(24), 5457 (2011).
[12]S. Wang and N. Ye, J. Am. Chem. Soc. **133**(30), 11458 (2011); S. Wang, N. Ye, W. Li, and D. Zhao, J. Am. Chem. Soc. **132**(25), 8779 (2010); H. Huang, L. Liu, S. Jin, W. Yao, Y. Zhang, and C. Chen, J. Am. Chem. Soc. **135**(49), 18319 (2013).
[13]H. Huang, J. Yao, Z. Lin, X. Wang, R. He, W. Yao, N. Zhai, and C. Chen, Angew. Chem., Int. Ed. Engl. **50**(39), 9141 (2011).
[14]C. Chen, Y. Wang, B. Wu, K. C. Wu, W. Zeng, and L. Yu, Nature **373** (6512), 322 (1995).
[15]S. Zhao, P. Gong, L. Bai, X. Xu, S. Zhang, Z. Sun, Z. Lin, M. Hong, C. Chen, and J. Luo, Nat. Commun. **5**, 4019 (2014).
[16]Y. S. Oseledchik, A. L. Prosvirnin, A. I. Pisarevskiy, V. V. Starshenko, V. V. Osadchuk, S. P. Belokrys, N. V. Svitanko, A. S. Korol, S. A. Krikunov, and A. F. Selevich, Opt. Mater. **4**(6), 669 (1995).
[17]A. G. Al-Ama, E. L. Belokoneva, S. Y. Stefanovich, O. V. Dimitrova, and N. N. Mochenova, Crystallogr. Rep. **51**(2), 225 (2006); H. Wu, S. Pan, K. R. Poeppelmeier, H. Li, D. Jia, Z. Chen, X. Fan, Y. Yang, J. M. Rondinelli, and H. Luo, J. Am. Chem. Soc. **133**(20), 7786 (2011); M. Zhang, S. Pan, X. Fan, Z. Zhou, K. R. Poeppelmeier, and Y. Yang, CrystEngComm **13**(8), 2899 (2011).
[18]H. Wu, S. Pan, H. Yu, D. Jia, A. Chang, H. Li, F. Zhang, and X. Huang, CrystEngComm **14**(3), 799 (2012).
[19]M. Zhang, X. Su, S. Pan, Z. Wang, H. Zhang, Z. Yang, B. Zhang, L. Dong, Y. Wang, F. Zhang, and Y. Yang, J. Phys. Chem. C **118**(22), 11849 (2014).
[20]P. N. Butcher and T. P. McLean, Proc. Phys. Soc. **81**, 219 (1963); D. Aspnes, Phys. Rev. B **6**(12), 4648 (1972); E. Ghahramani, D. Moss, and J. Sipe, Phys. Rev. B **43**(11), 8990 (1991); Z. Levine and D. Allan, Phys. Rev. Lett. **66**(1), 41 (1991); J. Sipe and E. Ghahramani, Phys. Rev. B **48** (16), 11705 (1993); A. Dal Corso and F. Mauri, Phys. Rev. B **50**(8), 5756 (1994); Z. Levine, Phys. Rev. B **49**(7), 4532 (1994).
[21]C. Aversa and J. Sipe, Phys. Rev. B **52**(20), 14636 (1995).
[22]S. N. Rashkeev, W. R. L. Lambrecht, and B. Segall, Phys. Rev. B **57**(7), 3905 (1998).
[23]J. Lin, M.-H. Lee, Z.-P. Liu, C. Chen, and C. J. Pickard, Phys. Rev. B **60**(19), 13380 (1999).
[24]C.-S. Li, M.S. thesis, Tamkang University, 2011.
[25]See supplementary material at http://dx.doi.org/10.1063/1.4906427 for the calculation details, the cutting radius of specific ion, calculated polarizabilities, and the Sellmeier coefficients derived from the measured and calculated refractive indices.
[26]S. J. Clark, M. D. Segall, C. J. Pickard, P. J. Hasnip, M. I. J. Probert, K. Refson, and M. C. Payne, Z. Kristallogr. **220**(5/6/2005), 567 (2005).
[27]A. M. Rappe, K. M. Rabe, E. Kaxiras, and J. D. Joannopoulos, Phys. Rev. B **41**(2), 1227 (1990); J. Lin, A. Qteish, M. Payne, and V. Heine, Phys. Rev. B **47**(8), 4174 (1993); M.-H. Lee, Ph.D. thesis, The University of Cambridge, 1996.
[28]J. P. Perdew, K. Burke, and M. Ernzerhof, Phys. Rev. Lett. **77**(18), 3865 (1996).
[29]M. J. Xia, B. Xu, and R. K. Li, J. Cryst. Growth **404**, 65 (2014).
[30]M.-H. Lee, C.-H. Yang, and J.-H. Jan, Phys. Rev. B **70**(23), 235110 (2004).
[31]C.-H. Lo, M.S. thesis, Tamkang University, 2005.
[32]R. French, J. Ling, F. Ohuchi, and C. Chen, Phys. Rev. B **44**(16), 8496 (1991); B. Zhang, Z. Yang, Y. Yang, M.-H. Lee, S. Pan, Q. Jing, and X. Su, J. Mater. Chem. C **2**(21), 4133 (2014).
[33]C.-G. Duan, J. Li, Z.-Q. Gu, and D.-S. Wang, Phys. Rev. B **60**(13), 9435 (1999).
[34]M. J. Frisch, G. W. Trucks, H. B. Schlegel, G. E. Scuseria, M. A. Robb, J. R. Cheeseman, G. Scalmani, V. Barone, B. Mennucci, G. A. Petersson *et al. Gaussian 09, Revision D.01* (Gaussian, Inc., Wallingford CT, 2009).
[35]J. P. Mathieu, *Optics: International Series of Monographs in Natural Philosophy* (Pergamon Press, Oxford, 1975).